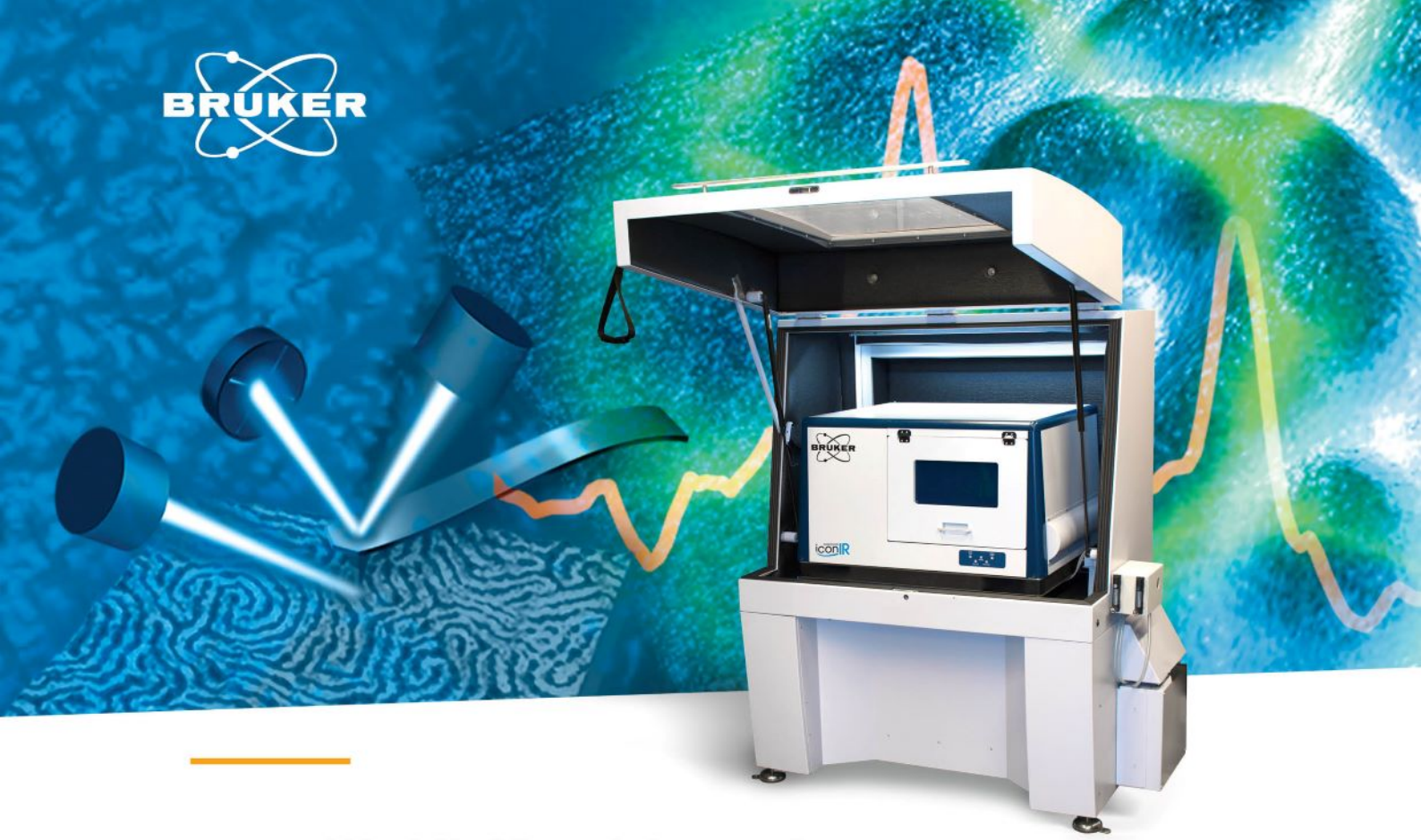

World's Most Advanced Photothermal IR Spectroscopy Solutions

Bruker's nanoscale infrared (nanoIR) spectrometers measure spatially varying physical and chemical properties in a diverse range of fields, from polymers and 2D materials to life science and micro-electronics. Fueling an impressive and growing publication record, these systems are advancing academic discovery and helping industrial companies solve critical process problems.

Proprietary spectroscopy and AFM technology:

- **NEW** Dimension IconIR large-sample system with PeakForce property mapping
- High-performance nanoIR spectroscopy with accurate and repeatable FTIR correlation
- Sub-10nm chemical resolution and monolayer sensitivity
- **NEW** Surface Sensitive AFM-IR mode with chemical probing depth to tens of nanometers

Take your materials research to the next level.
Visit www.bruker.com/nanoIR, email productinfo@bruker.com or call +1.408.376.4040/866.262.4040 for more information today.

Innovation with Integrity

Received: 4 October 2022 | Revised: 10 April 2023 | Accepted: 15 April 2023

DOI: 10.1002/app.54052

RESEARCH ARTICLE

Applied Polymer Science WILEY

Nickel hydroxide growth on renewable activated carbon microfibers for the development of supercapacitors

John Hinkle III[1,2] | Archana Bansode[1,2] | Nima Alizadeh[1,2] | Amulya Poudyal[2] | John Thornhill[2] | Anthony Bass[2] | Xinyu Zhang[1,2] | Andrew J. Adamczyk[2] | Thomas Elder[3] | Maria L. Auad[1,2]

[1]Center for Polymers and Advanced Composites, Auburn University, Auburn, Alabama, USA

[2]Department of Chemical Engineering, Auburn University, Auburn, Alabama, USA

[3]USDA-Forest Service, Southern Research Station, Auburn, Alabama, USA

Correspondence
Maria L. Auad, Center for Polymers and Advanced Composites, Auburn University,
Email: auad@auburn.edu

Funding information
NSF Crest, Grant/Award Number: 1735971; USDA-Forest Service, Grant/Award Number: 18-JV-11330131-073

Abstract

Lignin is one of the most common naturally occurring macromolecules. It is associated with cellulose and hemicelluloses in terrestrial plants, providing mechanical stiffness and contributing to moisture control and defense toward insects and fungi. Lignin is typically a polymer of three different cinnamyl alcohols, *para*-coumaryl alcohol, coniferyl alcohol, and sinapyl alcohol, which varies with the plant species. Solubilized lignin from the kraft pulping process is mainly concentrated and burned as part of the liquor recovery cycle in the kraft pulping. Given its aromatic nature, other uses of lignin include the development of platform chemicals, polymers, and fuels. This work uses lignin to develop carbon fibers to act as supercapacitors. Lignin microfibers were produced using an electrospinning process, carbonized under an inert atmosphere, and activated to increase surface area and improve capacitance. The activation process is shown to improve the specific capacitance of the material. In addition to activation, nanocrystals were grown on the surface of the carbon microfibers as these nanocrystals have been shown to improve the specific capacitance. When both surface modifications are performed to the lignin-based carbon fiber, it improves the specific capacitance retention regarding scan rate increase during cyclic voltammetry. The specific capacitance for the carbon fiber, activated carbon fiber, $Ni(OH)_2$ carbon fiber, and $Ni(OH)_2$ activated carbon fiber at 10 mV/s are 189, 206, 10, and 103 F/g.

KEYWORDS

activation, BET, carbon fibers, carbonization, cyclic voltammetry, electrospinning, lignin, microfibers, $Ni(OH)_2$ nanocrystals, supercapacitor

1 | INTRODUCTION

Supercapacitors are electrochemical devices that bridge traditional batteries and capacitors by providing better power density than a battery and energy density than a capacitor. As a result, supercapacitors can charge more quickly than a battery and discharge over a greater period of time than a capacitor. Among the different types of supercapacitors, the electrical double-layered capacitor uses high surface area materials, such as carbon fibers, as electrodes.[1,2]

Carbon fiber is known for its low density and high strength making it a valuable material for developing composites.[3,4] These properties are the reason why there

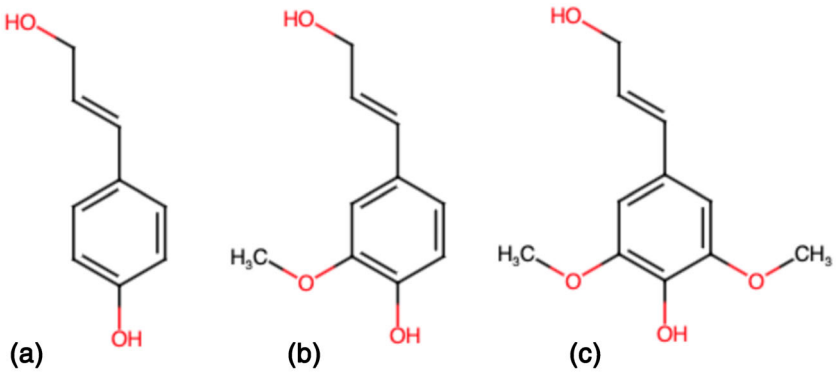

FIGURE 1 Lignin precursors. (a) *p*-coumaryl alcohol; (b) coniferyl alcohol; (c) sinapyl alcohol. [Color figure can be viewed at wileyonlinelibrary.com]

is a large demand for the material as well as the market size increasing yearly.[5] However, 90% of the carbon fiber produced worldwide utilizes polyacrylonitrile (PAN), a non-renewable material, as its precursor.[6] With the increasing concern on the use of non-renewable materials, research has expanded to find alternative sources for current materials. One such alternative source of carbon fiber is lignin.[7,8]

Lignin is one of the most common naturally occurring polymers, second only to cellulose.[9] It is a phenylpropanoid polymer, typically composed of three different monomers: *p*-coumaryl alcohol, coniferyl alcohol, and sinapyl alcohol.[10] Figure 1 shows the three different monomers that make up lignin.

The monomer composition of lignin changes based on the source of lignin. For example, angiosperm-based lignin is made of coniferyl alcohol and sinapyl alcohol; the ratios vary with species, while lignin from gymnosperms is made primarily of coniferyl alcohol.[11] In addition to differences based on the plant species, differences in the method by which lignin is isolated will also alter its properties. Some examples of isolated lignin include kraft lignin, alkaline lignin, and organosolv lignin.[12–14]

The alkaline lignin that is utilized in this paper was produced from sulfite lignin made from both angiosperm and gymnosperm trees. The sulfite lignin is dealkylated to partially remove the sulfur present before being treated again to increase its pH. This process makes the lignin water-soluble.[15]

Lignin has several practical applications that have been extensively examined, such as the production of vanillin, which is used as a flavoring agent, phenolic resins, or composites.[16–18] Lignin has also been reported as an economical, renewable carbon fiber precursor. Nippon Kayako Co. utilized lignosulphonates to produce carbon fiber on a commercial scale while reducing CO_2 emissions of the refinery plant.[16] Sudo et al. showed that steam-exploded lignin could have its aliphatic groups removed to produce mechanically strong carbon fiber.[19] Kubo et al. used lignin and a variety of synthetic polymers to extrude lignin fibers that were then carbonized.[20] Mainka et al. analyzed lignin-based carbon fibers for their potential use in the automotive industry.[21]

Among the methods for utilizing lignin fibers as a precursor for carbon fibers, the electrospinning process is one of the most novel.[22] This process uses a high voltage difference between a polymeric solution and a collection plate to produce nanofibers and microfibers. Electrospinning has been used to make fibers from several different polymers, such as polylactic acid, polycaprolactone, and polyethylene oxide.[23–26] In this technique, an electrically charged polymeric solution is collected at an oppositely charged metal plate, causing the solvent to be removed resulting in fibers being produced.[23]

One of the benefits of these carbon fibers is that they have a high surface area. The increased surface area corresponds with a good specific capacitance of the fiber. Specific capacitance is the intrinsic capacitance of a material, and capacitance is the ability of a material to hold a charge.[27]

In order to improve the specific capacitance of the material, there are various methods to increase the surface area. This is important as there is a correlation between increasing the surface area of a material and the specific capacitance.[28] One such method is called activation, which is known to improve the specific capacitance of carbon fiber through the increase in the surface area through either a physical or chemical processes.[29,30] In addition to activation, surface properties can be improved by growing nickel hydroxide $Ni(OH)_2$ crystals into fibers.[31]

In the literature, lignin nanofibers that have been produced using the electrospinning process have successfully been carbonized to form carbon nanofibers with excellent properties for electrochemical applications.[22,32,33] However, these electrochemical properties can be further improved through the previously mentioned methods.

This work will show that carbonizing electrospun lignin microfibers can produce electrochemical capacitors. In addition, this work will show how combining different surface modifications will improve not only specific capacitance, but also how the specific capacitance retention is improved

FIGURE 2 Electrospinning setup. [Color figure can be viewed at wileyonlinelibrary.com]

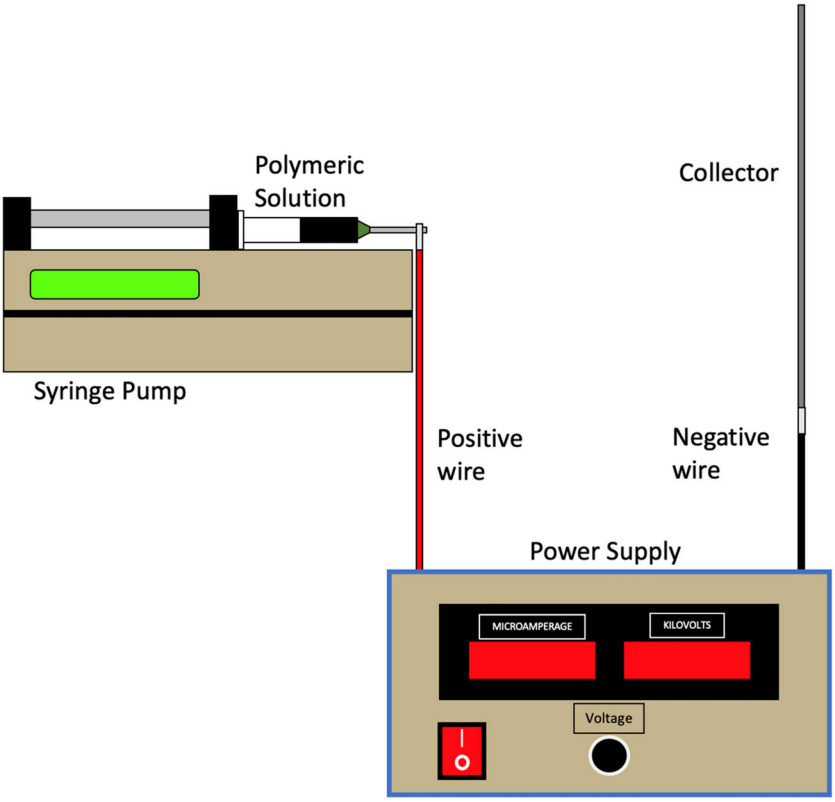

TABLE 1 Final electrospinning parameters.

Parameters	Value
Voltage	14 kV
Flow Rate	1.0 mL/h
Distance	10 cm

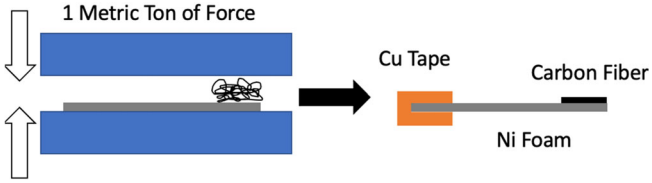

FIGURE 3 Capacitor development. [Color figure can be viewed at wileyonlinelibrary.com]

with the increase of scanning rates for this renewable form of carbon fiber. The material that is produced could become a potential source of renewable carbon fiber with the potential of surface modification for supercapacitors replacing traditional materials on the market.

2 | MATERIALS AND METHODS

Alkaline lignin was purchased from Tokyo Chemical Industry. Sodium hydroxide and potassium hydroxide were acquired from VWR, polyethylene oxide (M.W. 400,000) was purchased from Scientific Polymer Productions, Inc., nickel(II) nitrate hexahydrate was purchased from Alfa Aesar, ethyl alcohol 200 proof was bought from Pharmaco-Aaper, nickel foam was purchased from KUNHEWUHUA, and urea was provided Auburn University College of Agriculture who had acquired it from Piedmont Fertilizer Company.

TABLE 2 Cyclic voltammetry parameters.

Parameters	Values
Voltage difference	−0.9 to 0.1 V
Scan rate	10, 20, 50, 100, 150, and 200 mV/s
Number of cycles	2
Mass	15.0 mg

2.1 | Electrospinning

A solution was made with 25 mL of distilled water, 2.5 g of alkaline lignin, 0.278 g of polyethylene oxide (PEO), and 0.75 g of sodium hydroxide (NaOH). This solution was based on a method reported by Hu et al.[22] The solution is added to a 10 mL syringe with a 21-gauge flat tip

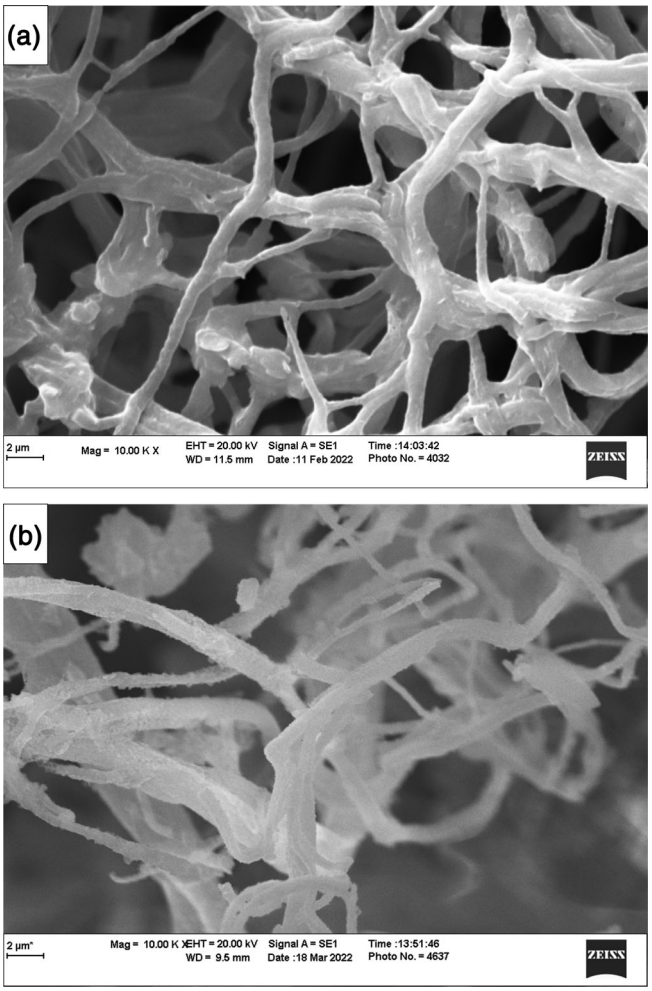

FIGURE 4 (a) Electrospun lignin microfibers; (b) carbonized lignin microfibers.

needle and is loaded into a syringe pump. A positive wire was attached to the needle, and the ground was placed on the metal plate, which acted as the collector. These wires are connected to a high voltage generator. This setup can be seen in Figure 2.

Table 1 shows the final parameters used during the electrospinning process. These parameters were selected by the quality of electrospun fiber produced as determined by a scanning electron microscopy (SEM) analysis based on uniformity and lack of droplets present in the fibers.

The lignin microfibers produced by electrospinning were placed into a porcelain crucible and loaded into a Thermo Scientific Lindberg Blue M tube furnace. Nitrogen was used to purge the furnace to prevent atmospheric oxygen from reacting with the lignin fibers. The furnace was heated to 105°C at a rate of 10°C min^{-1} and was held isothermally for 30 min. The temperature was then increased to 850°C at a rate of 10°C min^{-1} and was held isothermally for 30 min. The material was then allowed to

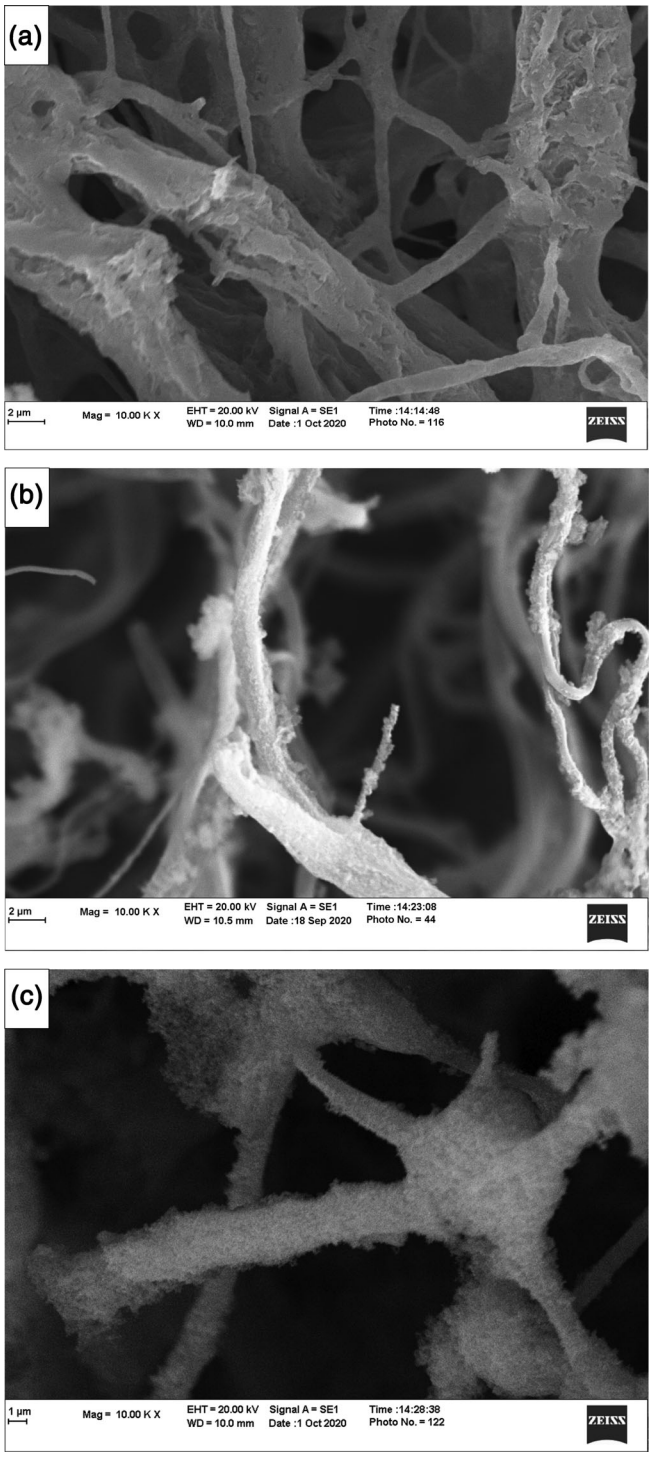

FIGURE 5 (a) Activated carbon microfiber, (b) $Ni(OH)_2$ non-activated carbon microfiber, and (c) $Ni(OH)_2$ activated carbon microfiber.

cool under ambient conditions. This process was based on the work published by Hu et al.[22]

Activation of the carbon fibers produced in the previous step was accomplished by treating the carbon fibers with a 1 M solution of potassium hydroxide. Next, the fibers were heated in the furnace using the protocol

TABLE 3 Surface area and pore volume of carbon fiber.

Sample	Surface area ($m^2\ g^{-1}$)	Pore surface area ($m^2\ g^{-1}$)	Pore diameter (nm)	Total pore volume ($cm^3\ g^{-1}$)
Base carbon fiber	474.386	60.590	3.421	$3.645*10^{-1}$
$Ni(OH)_2$ carbon fiber	156.239	49.728	3.132	$2.064*10^{-1}$
Activated carbon fiber	795.392	306.20	2.970	$7.436*10^{-1}$
$Ni(OH)_2$ activated carbon fiber	2156.23	1226.1	3.938	$2.562*10^{-0}$

described in the previous paragraph for the initial carbonization.

Samples of both activated and non-activated carbon microfibers were treated in a solution consisting of 500 mg of urea, 20 mL of water, 20 mL of ethanol, and 1.16 g of $Ni(NO_3)_2{\cdot}6H_2O$. The beaker containing the fibers and treatment solution was then placed in an oil bath at 70°C for 15 h, after which the fibers were dried in a VWR 1430 M Vacuum Oven under 60 cm Hg vacuum at 60°C for 2 h.[31]

All forms of fibers produced during these experiments were visually inspected by a Zeiss Evo 50 Scanning Electron Microscope with an electron high tension (EHT) of 20.0 kV; the samples were sputter-coated with gold nanoparticles under an argon atmosphere for the analysis.

A Brunauer–Emmett–Teller analysis (BET analysis) was performed using an Anton Parr Autosorb IQ TPX to quantify the samples surface area and pore volume of all carbon fiber samples. The samples were loaded into a glass adsorption cell in the BET and degassed at 200°C for 19 h under 75.995 cm Hg vacuum, after which the enclosure was backfilled with helium until the analysis was performed. The samples underwent a standard N_2 adsorption test at 77 K. The total pore volume was calculated by the last data point during the adsorption portion of the test. The surface area is calculated between 0.05 and 0.3 P/P_o. The adsorption portion of the test calculated pore surface area. The ASiQwin program, which is provided by Anton Parr, was used for the purpose of analyzing the BET data.

2.2 | Specimen preparation

Capacitors were developed from each carbon fiber sample by placing the carbon fiber onto the bottom of a rectangular piece of nickel foam. The foam and carbon fiber were then placed between two metal plates covered with Teflon to prevent sticking and placed onto a hydraulic press that applied 1 ton-force onto the plates, causing a physical attachment between the carbon fiber and the nickel foam. Lastly, copper tape is applied to the end of the nickel foam opposite of the carbon fiber for an alligator clip to be attached to the capacitor for testing. Figure 3 shows the specimen prepared using this method.

2.3 | Cyclic voltammetry analysis

To calculate the specific capacitance, the capacitors were loaded into a three-electrode cell. The electrolyte used was 6 M KOH, the reference electrode was a Hg/HgO electrode, and the counter electrode was a platinum wire. The capacitor acts as the working electrode. Cyclic voltammetry was performed using a Gamry Instruments Interface 1000 Potentiostat/Galvanostat/ZRA with Gamry Framework to operate the apparatus and Gamry Echem Analyst to analyze the data. Table 2 shows the parameters used in the cyclic voltammetry test. These voltage differences were determined through a prior experiment where the voltage range was between −1 and 1 volt. The ranges shown in Table 2 were selected as these were the ranges that had the least amount of reduction–oxidation peaks from occurring in the previous experiment, as evident due to the lack of peaks present in the cyclic voltammetry graphs is undesirable in supercapacitors. This process is based on a procedure reported by Denmark et al.[34]

After the cyclic voltammetry test, the data was plotted using Origin 2019 64 bit. To determine the specific capacitance of a given capacitor, the mathematical integral of one cycle was taken, and Equation (1) was used to calculate the specific capacitance.[35]

$$\text{Specific Capcitance} = \frac{\int_{V_1}^{V_2} I\mathrm{dV}}{(\nu * m * \Delta V)} \quad (1)$$

V = Voltage; I = Amperage; ν = scan rate; m = mass.

3 | RESULTS AND DISCUSSION

3.1 | Fiber production

The electrospinning of the lignin-based solution was successful in producing microfibers. Figure 4 shows the SEM images of the resulting fibers before carbonization and after carbonization. These fibers are nonwoven and have

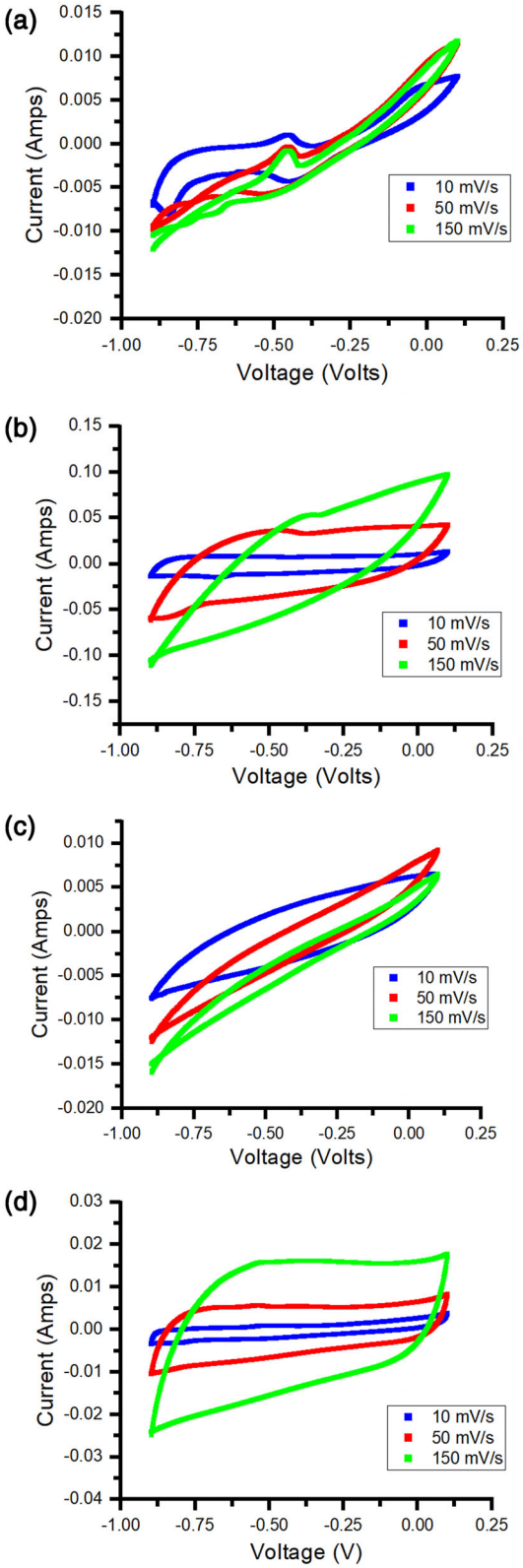

FIGURE 6 (a) Cyclic voltammetry of carbon fiber, (b) cyclic voltammetry of activated carbon fiber, (c) cyclic voltammetry of $Ni(OH)_2$ carbon fiber, and (d) cyclic voltammetry of $Ni(OH)_2$ activated carbon fiber. [Color figure can be viewed at wileyonlinelibrary.com]

diameters of 1.18 ± 0.42 and 1.79 ± 1.05 μm, respectively. It can be seen that after carbonization, the fibrous morphology is retained.

Based on the images in Figure 5, the different treatments have substantially modified the surfaces of the fibers. For the activated fibers, the roughness of the fibers has increased based on a visual inspection.[36] In addition to the activation, the effect of $Ni(OH)_2$ addition can be seen with the crystalline growth on the fibers, as confirmed by the SEM. The fiber diameters remain similar to the previous two samples with the average fiber diameter being 1.14 ± 0.74, 0.849 ± 0.58, and 1.49 ± 0.62 μm for activated carbon fiber, $Ni(OH)_2$ carbon fiber, and $Ni(OH)_2$ activated carbon fiber, respectively. All samples were continuous, nonwoven fabrics before carbonization as well as after carbonization and the two different surface treatments.

Table 3 shows the surface area, pore surface area, and pore volume for the different carbon fibers collected from the BET analysis performed on our samples.

From the analysis, the base carbon fibers have a high surface area. The surface decreased, along with the pore surface area and total pore volume, with the $Ni(OH)_2$ addition. The $Ni(OH)_2$ crystal growth is causing the smoother surface, which would reduce the surface area, pore surface area, and pore volume. However, upon activation of the base carbon fiber, there is an increase in all three results. Due to the activated carbon fiber having more nucleation sites for the $Ni(OH)_2$ growth compared to the base carbon fiber, the crystals to grow independently and unevenly thus forming a rougher surface.

Cyclic voltammetry tests were performed on the resulting capacitors, and the results can be observed in Figure 6.

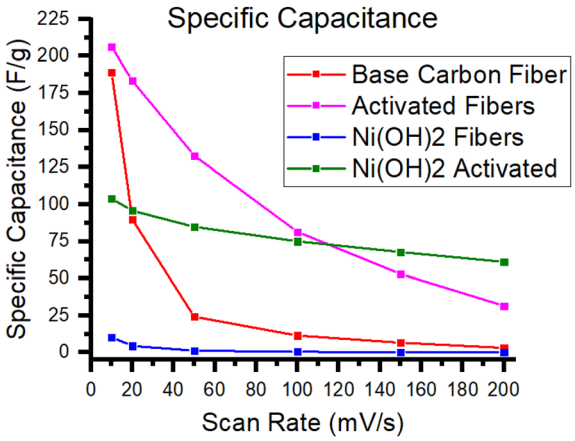

FIGURE 7 The specific capacitance of base carbon fiber, activated carbon fiber, $Ni(OH)_2$ carbon fibers, and $Ni(OH)_2$ activated carbon fibers. [Color figure can be viewed at wileyonlinelibrary.com]

It can be seen in Figure 6 that the different pretreatments have a substantial effect on the electrochemical properties of the resulting material. The base carbon fiber shows poor capacitor-like behavior, as indicated by the reduction–oxidation peaks present in the cyclic voltammetry graph. However, the reduction–oxidation peaks are no longer present when the material is activated or treated with $Ni(OH)_2$. The significant difference between these two samples is the charge that is built up in the material, which is the area within the curve as defined by Equation (1).[35] The sample that shows the best capacitor-like behavior is the $Ni(OH)_2$ activated carbon fiber. The $Ni(OH)_2$ activated carbon fiber is the most like an ideal capacitor due to its rectangular-like shape, as the theoretical ideal capacitor would appear as a rectangle in a cyclic voltammetry test.[37]

Utilizing Equation (1), each of the cyclic voltammetry graphs was analyzed to produce the specific capacitance of each sample for each scan rate at which they were tested. The specific capacitance results can be seen in Figure 7.

The data shows the change in cyclic voltammetry based on the different pretreatments. The highest specific capacitance that was observed was from the activated carbon fiber, which had a specific capacitance of 206 F/g at 10 mV/s, with the base carbon fiber at 189 F/g at 10 mV/s.

The $Ni(OH)_2$ carbon fiber had the worst performance out of the four samples, with the lowest specific capacitance at every scan rate tested. This was not predicted initially as $Ni(OH)_2$ has improved specific capacitance, as shown by Zhang et al.[31] Therefore, it is proposed that the non-activated $Ni(OH)_2$ carbon fibers were covered by $Ni(OH)_2$ as evidenced by the reduction of the pore surface area, which prevented surface interaction between the electrolyte and the carbon fiber, reducing the specific capacitance. This theory is consistent with the BET results, which showed a reduction in the surface area, pore surface area, and total pore volume.

Of the three modified samples, the activated carbon fiber and the $Ni(OH)_2$ activated carbon fiber showed improvements over the base carbon fiber. At every scan rate, the activated carbon fiber had a higher specific capacitance than the base carbon fiber. The $Ni(OH)_2$ activated carbon fiber had a higher specific capacitance at every scan rate except for the 10 mV/s. Both samples have differing advantages. When a lower scan rate was used, the activated carbon fibers had a higher specific capacitance. In contrast, at the higher 150 and 200 mV/s scan rates, the $Ni(OH)_2$ activated carbon fiber shows a higher result. In addition, the $Ni(OH)_2$ activated carbon fiber showed better specific capacitance retention over the various scan rates, with a 58.8% retention compared to the activated carbon fiber 15.3% retention over the various scan rates.

4 | CONCLUSIONS

Through electrospinning, lignin microfibers were successfully produced. These fibers served as the precursor for carbon microfibers. These carbon fibers were subjected to both an activation treatment to increase surface area and the growth of $Ni(OH)_2$ nanocrystals onto the fibers. The activated and $Ni(OH)_2$ activated carbon fiber showed improvements compared to the base carbon fiber either through improved specific capacitance or improved specific capacitance retention. This shows the different effects of the various surface treatments and how combining the different surface treatments can produce results that differ from the individual surface treatments. By combining the different surface treatments, the renewable carbon fiber that was produced in this study can have its electrochemical properties tailored to fit the desired properties; either a high specific capacitance at low scan rates, or the ability to have a good specific capacitance over various scan rates.

AUTHOR CONTRIBUTIONS

John Hinkle: Conceptualization (equal); data curation (equal); methodology (equal); writing – original draft (equal); writing – review and editing (equal). **Archana Bansode:** Investigation (supporting). **Nima Alizadeh:** Investigation (supporting). **Amulya Poudyal:** Investigation (supporting). **John Thornhill:** Investigation (supporting). **Anthony Bass:** Investigation (supporting). **Xinyu Zhang:** Investigation (supporting); methodology (supporting). **Andrew J. Adamczyk:** Investigation (supporting); methodology (supporting); writing – review and editing (supporting). **Thomas Elder:** Conceptualization (supporting); funding acquisition (equal); methodology (supporting); project administration (supporting); resources (supporting); supervision (supporting); writing – review and editing (supporting). **Maria Auad:** Conceptualization (lead); funding acquisition (lead); investigation (lead); project administration (lead); resources (lead); supervision (lead).

ACKNOWLEDGMENTS

This project was supported by the NSF Crest Grant 1735971 and the USDA-Forest Service Grant 18-JV-11330131-073. We also wanted to thank Dr. Ramsis Farag and Dr. Rohit Kanungo for assisting at the beginning of this project. In addition, we would also like to thank Gautam Chandrasekhar and Dr. Vijaya Rangari for assisting with characterization of the material.

DATA AVAILABILITY STATEMENT

The data that support the findings of this study are available from the corresponding author upon reasonable request.

ORCID

Maria L. Auad https://orcid.org/0000-0001-6932-5645

REFERENCES

[1] A. González, E. Goikolea, J. A. Barrena, R. Mysyk, *Renew. Sustain. Energy Rev.* **2016**, *58*, 1189.
[2] Y. Xie, *Fib. Polym.* **2021**, *23*, 10.
[3] S.-Y. Fu, B. Lauke, E. Mäder, C.-Y. Yue, X. Hu, *Compos. Part A: Appl. Sci. Manuf.* **2000**, *31*, 1117.
[4] Q. Zhang, J. Liu, R. Sager, L. Dai, J. Baur, *Compos. Sci. Technol.* **2009**, *69*, 594.
[5] *Carbon fiber market Size, share and GROWTH: Industry REPORT 2021 to 2026 WITH COVID impact – Mordor intelligence*. Carbon Fiber Market Size, Share and Growth | Industry Report 2021 to 2026 With COVID Impact – Mordor Intelligence. Retrieved January 21, 2022 from https://www.mordorintelligence.com/industry-reports/carbon-fiber-market
[6] N. Yusof, A. F. Ismail, *J. Anal. Appl. Pyrol.* **2012**, *93*, 1.
[7] B. Lochab, I. K. Varma, J. Bijwea, *Adv. Mater. Phys. Chem.* **2012**, *02*, 221.
[8] Oak Ridge National Laboratory, A. L. Compere, W. L. Griffith, C. F. Leitten, J. T. Shaffer, *Low Cost Carbon Fiber from Renewable Resources*, Dept. of Energy, Washington, DC **2001**.
[9] D. Watkins, M. Nuruddin, M. Hosur, A. Tcherbi-Narteh, S. Jeelani, *J. Mater. Res. Technol.* **2015**, *4*, 26.
[10] J. Ralph, C. Lapierre, W. Boerjan, *Curr. Opin. Biotechnol.* **2019**, *56*, 240.
[11] A. Lourenço, H. Pereira, *Lignin – Trends and Applications*, IntechOpen, London, UK **2019**, essay.
[12] G. A. Smook, *Handbook for Pulp and Paper Technologists*, Tappi Press, Peachtree Corners, GA **2016**.
[13] C. Rutten, A. Ramírez, J. Posada Duque, *J. Chem. Technol. Biotechnol.* **2016**, *92*, 257.
[14] R. El Hage, N. Brosse, L. Chrusciel, C. Sanchez, P. Sannigrahi, A. Ragauskas, *Polym. Degrad. Stab.* **2009**, *94*, 1632.
[15] *Lignin* (*alkaline*). Lignin 8061-51-6 | Tokyo Chemical Industry Co.; Ltd. (APAC). Retrieved January 21, 2022 from https://www.tcichemicals.com/OP/en/p/L0082
[16] A. Agrawal, N. Kaushik, S. Biswas, *Scitech J.* **2014**, *1*, 30.
[17] D. Stewart, *Indust. Crops Prod.* **2008**, *27*, 202.
[18] T. Aro, P. Fatehi, *ChemSusChem* **2017**, *10*, 1861.
[19] K. Sudo, K. Shimizu, *J. Appl. Polym. Sci.* **1992**, *44*, 127.
[20] S. Kubo, J. F. Kadla, *J. Polym. Environ.* **2005**, *13*, 97.
[21] H. Mainka, O. Täger, E. Körner, L. Hilfert, S. Busse, F. T. Edelmann, A. S. Herrmann, *J. Mater. Res. Technol.* **2015**, *4*, 283.
[22] S. Hu, S. Zhang, N. Pan, Y.-L. Hsieh, *J. Power Sources* **2014**, *270*, 106.
[23] N. Bhardwaj, S. C. Kundu, *Biotechnol. Adv.* **2010**, *28*, 325.
[24] R. Casasola, N. L. Thomas, A. Trybala, S. Georgiadou, *Polymer* **2014**, *55*, 4728.
[25] J. Lannutti, D. Reneker, T. Ma, D. Tomasko, D. Farson, *Mater. Sci. Eng., C* **2007**, *27*, 504.
[26] J. Deitzel, *Polymer* **2001**, *42*, 8163.
[27] Encyclopædia Britannica Inc. Capacitance. Encyclopædia Britannica. n.d. Retrieved February 16, 2022, from https://www.britannica.com/science/capacitance
[28] E. Taer, A. Agustino, R. Farma, R. Taslim, P. M. Awitdrus, A. Ira, S. D. Yardi, Y. P. Sari, H. Yusra, S. Nurjanah, S. D. Hartati, Z. Aini, R. N. Setiadi, *J. Phys.: Conf. Ser.* **2018**, *1116*, 032040.
[29] J. Maciá-Agulló, B. Moore, D. Cazorla-Amorós, A. Linares-Solano, *Carbon* **2004**, *42*, 1367.
[30] C. Ruan, P. Li, J. Xu, Y. Chen, Y. Xie, *Inorg. Chem. Front.* **2019**, *6*, 3583.
[31] L. Zhang, Q. Ding, Y. Huang, H. Gu, Y.-E. Miao, T. Liu, *ACS Appl. Mater. Interf.* **2015**, *7*, 22669.
[32] J. Roman, W. Neri, A. Derré, P. Poulin, *Carbon* **2019**, *145*, 556.
[33] M. Zhu, H. Liu, Q. Cao, H. Zheng, D. Xu, H. Guo, S. Wang, Y. Li, J. Zhou, *ACS Sustain. Chem. Eng.* **2020**, *8*, 12831.
[34] I. Denmark, S. Macchi, F. Watanabe, T. Viswanathan, N. Siraj, *Electrochemistry* **2021**, *2*, 29.
[35] H. Z. Chi, Y. Li, Y. Xin, H. Qin, *Chem. Commun.* **2014**, *50*, 13349.
[36] Biolin Scientific. Surface roughness. Measurements. n.d. Retrieved January 21, 2022, from https://www.biolinscientific.com/measurements/surface-roughness
[37] D. Boonpakdee, C. F. Guajardo Yévenes, W. Surareungchai, C. La-o-vorakiat, *J. Mater. Chem. A* **2018**, *6*, 7162.

SUPPORTING INFORMATION

Additional supporting information can be found online in the Supporting Information section at the end of this article.

How to cite this article:
J. Hinkle III, A. Bansode, N. Alizadeh, A. Poudyal, J. Thornhill, A. Bass, X. Zhang, A. J. Adamczyk, T. Elder, M. L. Auad, *J. Appl. Polym. Sci.* **2023**, *140*(28), e54052. https://doi.org/10.1002/app.54052